

Exciting Quantized Vortex Rings in a Superfluid Unitary Fermi Gas

Aurel Bulgac
University of Washington

Collaborators: Michael M. Forbes (Seattle, now Washington State U-Pullman)
Yuan-Lung (Alan) Luo (Seattle)
Michelle M. Kelley (Urban-Champaign)
Piotr Magierski (Warsaw/Seattle)
Kenneth J. Roche (PNNL/Seattle)
Yongle Yu (Wuhan, PRC)
Gabriel Wlazlowski (Warsaw/Seattle)

Funding: DOE, NSF

Computing:
Athena UW Cluster → *Hyak UW cluster*,
Jaguar → *Titan, NCCS*

Original pptx slides with movies, a related talk given by M.M. Forbes and other related materials can be downloaded at

http://www.phys.washington.edu/users/bulgac/media_files/VR/

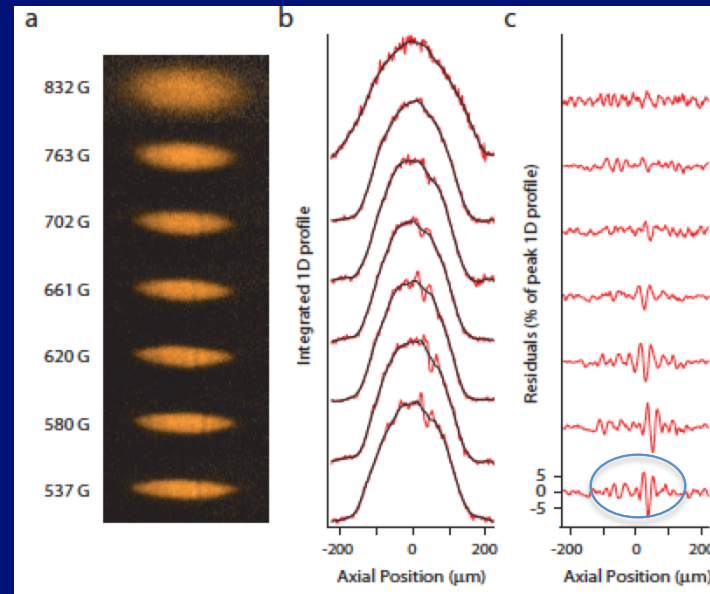
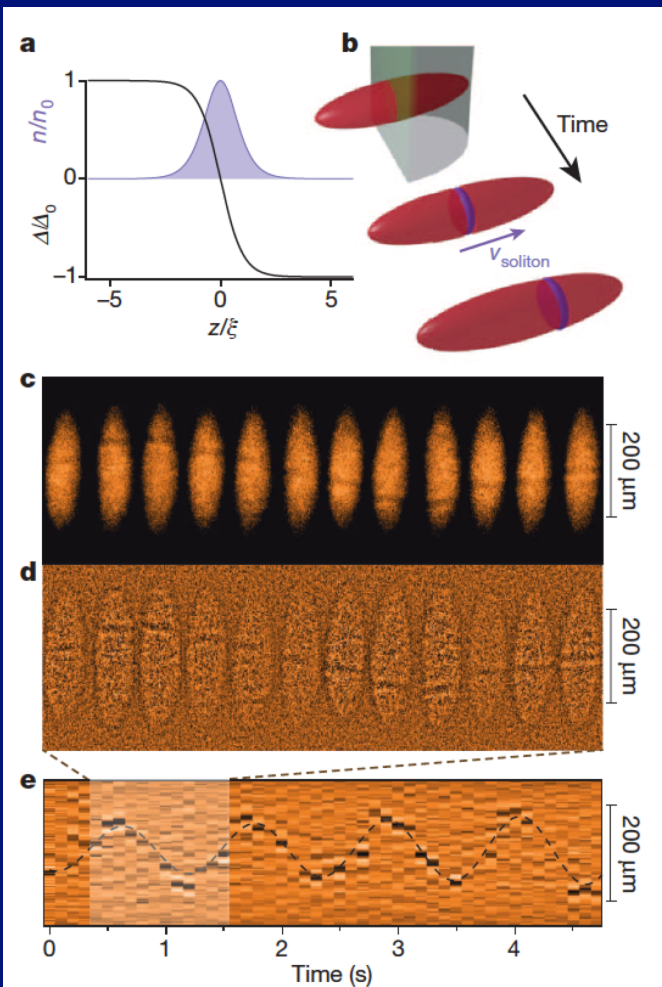
The Challenge put forward by experiment

Heavy solitons in a fermionic superfluid

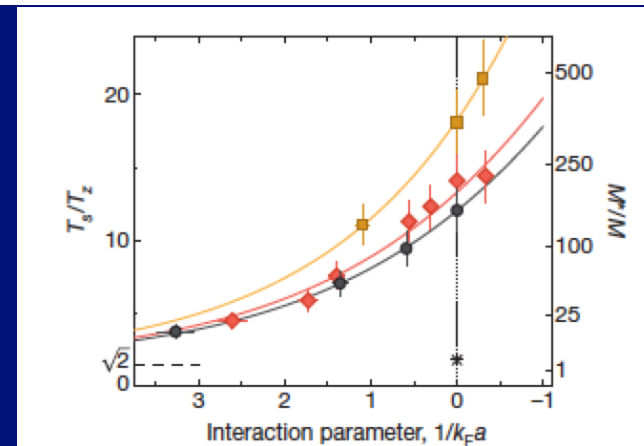
Tarik Yefsah¹, Ariel T. Sommer¹, Mark J. H. Ku¹, Lawrence W. Cheuk¹, Wenjie Ji¹, Waseem S. Bakr¹ & Martin W. Zwierlein¹

426 | NATURE | VOL 499 | 25 JULY 2013

Axially symmetric trap!

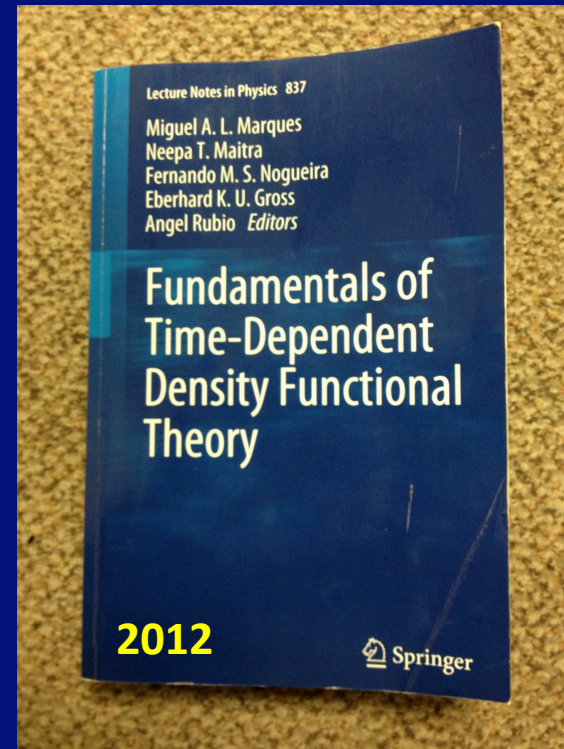
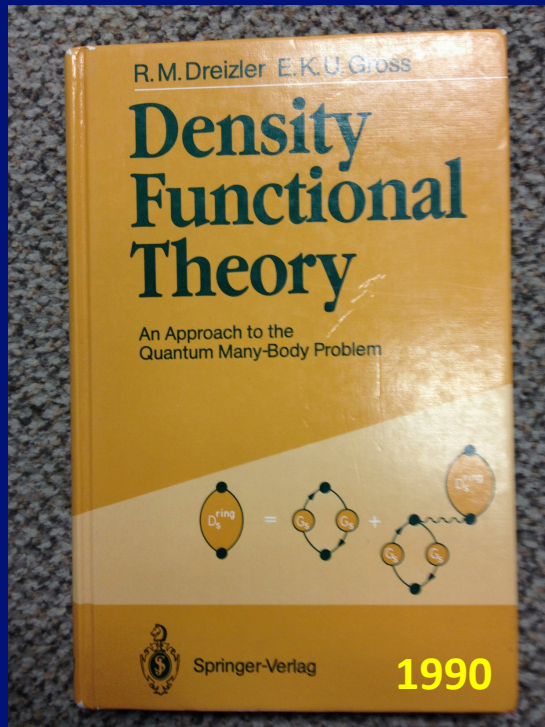


The observed "heavy solitons" are about ten times wider than a vortex core or domain wall (dark soliton)



The "heavy solitons" move about ten times slower than a domain wall (dark soliton)

Main Theoretical Tool

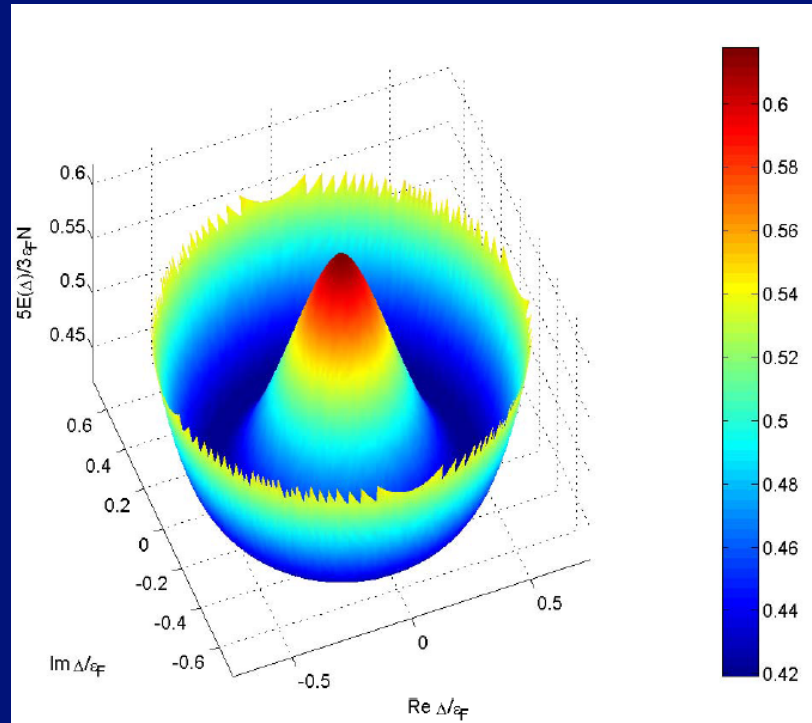


DFT has been developed and used mainly to describe normal (non-superfluid) electron systems

A new local extension of DFT to superfluid systems and time-dependent phenomena was developed

Review: A. Bulgac, *Time-Dependent Density Functional Theory and Real-Time Dynamics of Fermi Superfluids*, Ann. Rev. Nucl. Part. Sci. 63, 97 (2013)

Energy of a Fermi system as a function of the pairing gap



$$\dot{n} + \vec{\nabla} \cdot [\vec{v}n] = 0$$

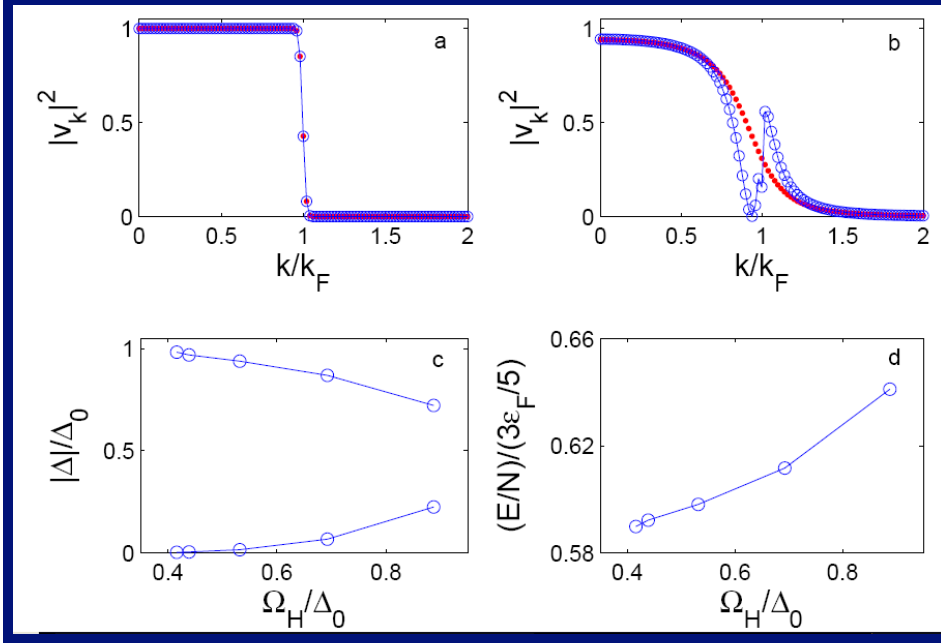
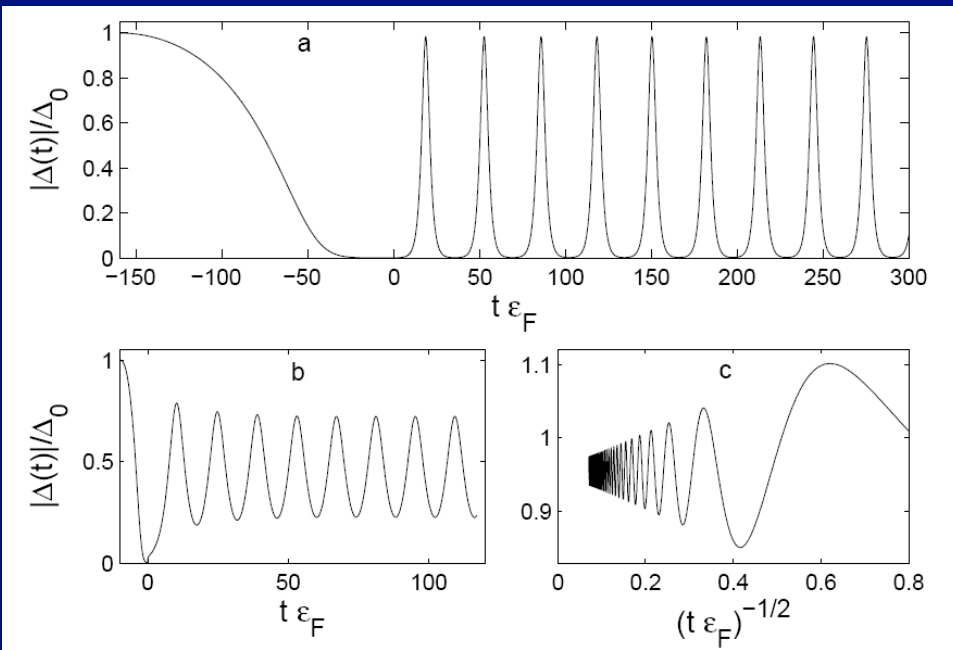
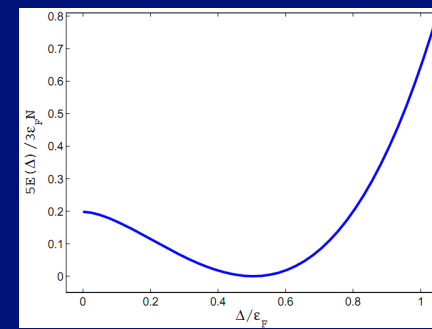
$$m\dot{\vec{v}} + \vec{\nabla} \cdot \left\{ \frac{m\vec{v}^2}{2} + \mu[n] \right\} = 0$$

$$i\hbar e^{i\gamma} \dot{\Psi}(\vec{r}, t) = -\frac{\hbar^2}{4m} \Delta \Psi(\vec{r}, t) + U(|\Psi(\vec{r}, t)|^2) \Psi(\vec{r}, t)$$

Landau's hydrodynamics
No Planck's constant!

Ginzburg-Landau-like equation

Response of a unitary Fermi system to changing the scattering length with time



- All these modes have a very low frequency below the pairing gap, a very large amplitude and very large excitation energy, and no spatial dependence
- None of these modes can be described either within two-fluid hydrodynamics or Ginzburg-Landau like approaches

What is Density Functional Theory?

$$\Psi(\vec{r}_1, \dots, \vec{r}_N, t) \Rightarrow n(\vec{r}, t)$$

Kohn-Sham theorem (1965)

$$H = \sum_i^N T(i) + \sum_{i<j}^N U(ij) + \sum_{i<j<k}^N U(ijk) + \dots + \sum_i^N V_{ext}(i)$$

$$H\Psi_0(1,2,\dots,N) = E_0\Psi_0(1,2,\dots,N)$$

$$n(\vec{r}) = \langle \Psi_0 | \sum_i^N \delta(\vec{r} - \vec{r}_i) | \Psi_0 \rangle$$

$$\Psi_0(1,2,\dots,N) \Leftrightarrow V_{ext}(\vec{r}) \Leftrightarrow n(\vec{r})$$

$$E_0 = \min_{n(\vec{r})} \int d^3r \left\{ \frac{\hbar^2}{2m^*(\vec{r})} \tau(\vec{r}) + \varepsilon[n(\vec{r})] + V_{ext}(\vec{r})n(\vec{r}) \right\}$$

$$n(\vec{r}) = \sum_i^N |\varphi_i(\vec{r})|^2, \quad \tau(\vec{r}) = \sum_i^N |\vec{\nabla} \varphi_i(\vec{r})|^2$$

**Injective map
(one-to-one)**

**Universal functional of particle density alone
Independent of external potential**

Normal Fermi systems only!

However, not everyone is normal!

The SLDA (DFT) energy density functional at unitarity for equal numbers of spin-up and spin-down fermions

Dimensional arguments, renormalizability, Galilean invariance, and symmetries (translational, rotational, gauge, parity) determine the functional (energy density)

$$\varepsilon(\vec{r}) = \frac{\hbar^2}{m} \left\{ \left[\alpha \frac{\tau_c(\vec{r})}{2} - \tilde{\Delta}(\vec{r}) v_c(\vec{r}) \right] + \beta \frac{3(3\pi^2)^{2/3} n^{5/3}(\vec{r})}{5} \right\} - \frac{\hbar^2}{m} (\alpha - 1) \frac{j^2(\vec{r})}{2n(\vec{r})}$$

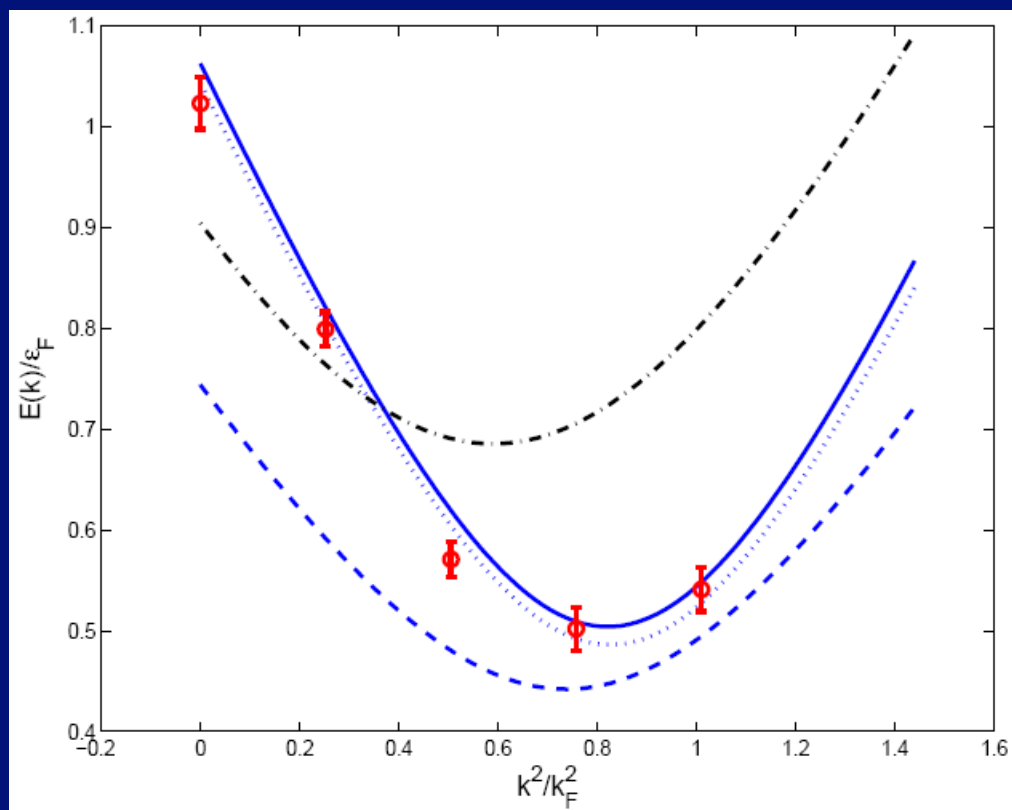
$$\Delta(\vec{r}) = \frac{\hbar^2}{m} \tilde{\Delta}(\vec{r})$$

$$n(\vec{r}) = 2 \sum_{0 < E_k < E_c} |v_k(\vec{r})|^2, \quad \tau_c(\vec{r}) = 2 \sum_{0 < E_k < E_c} |\vec{\nabla} v_k(\vec{r})|^2,$$

$$v_c(\vec{r}) = \sum_{0 < E < E_c} u_k(\vec{r}) v_k^*(\vec{r}) \quad \Leftarrow \text{divergent without a cutoff, need RG}$$

- Three dimensionless constants α , β , and γ (which enters in the definition of the pairing gap) determining the functional are extracted from QMC for homogeneous systems by fixing the total energy, the pairing gap and the effective mass
- SLDA has been verified and validated against a large number of quantum Monte Carlo results for inhomogeneous systems and experimental data as well

Quasiparticle spectrum in homogeneous matter

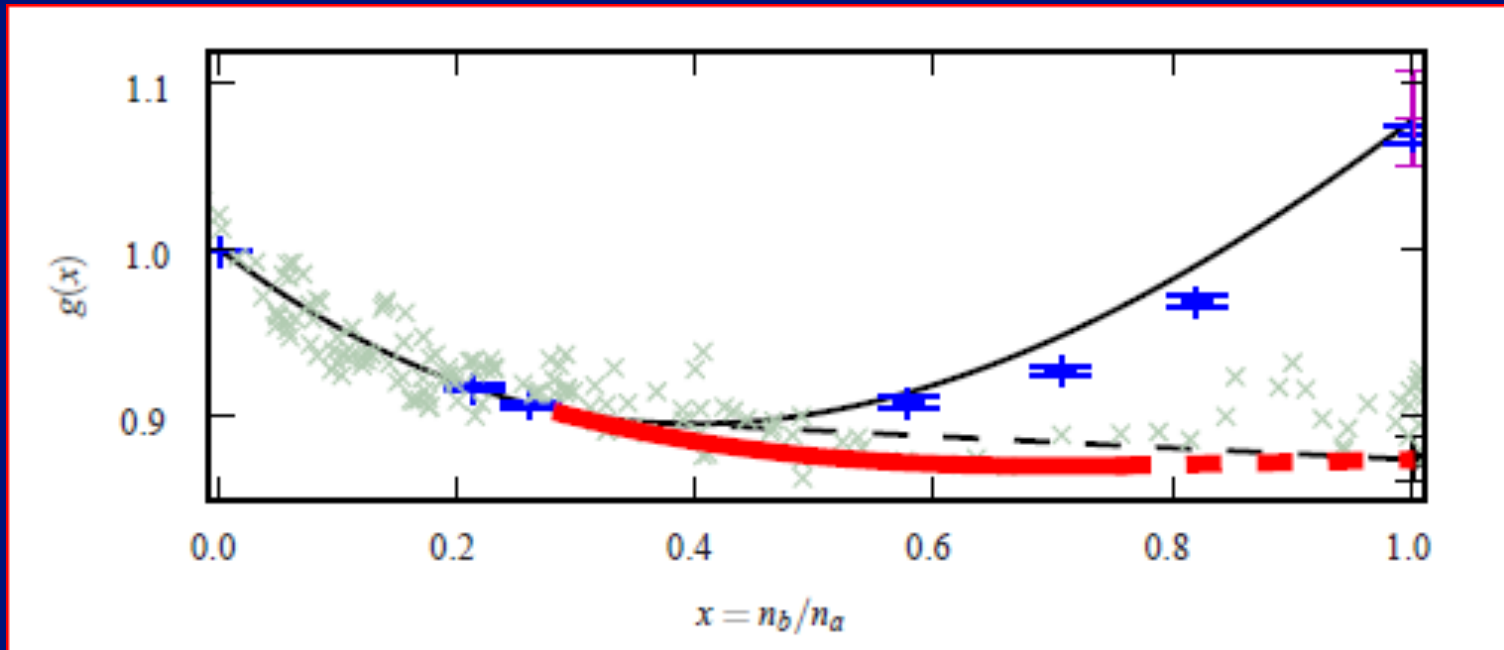


- solid/dotted blue line - SLDA based on homogeneous GFM due to Carlson *et al*
- red circles - GFM due to Carlson and Reddy
- dashed blue line - SLDA, homogeneous MC due to Juillet
- black dashed-dotted line - meanfield at unitarity

SLDA predictions vs Quantum Monte Carlo results for finite systems in traps

Normal State				Superfluid State			
(N_a, N_b)	$E_{FN\text{DMC}}$	$E_{AS\text{LDA}}$	(error)	(N_a, N_b)	$E_{FN\text{DMC}}$	$E_{AS\text{LDA}}$	(error)
(3, 1)	6.6 ± 0.01	6.687	1.3%	(1, 1)	2.002 ± 0	2.302	15%
(4, 1)	8.93 ± 0.01	8.962	0.36%	(2, 2)	5.051 ± 0.009	5.405	7%
(5, 1)	12.1 ± 0.1	12.22	0.97%	(3, 3)	8.639 ± 0.03	8.939	3.5%
(5, 2)	13.3 ± 0.1	13.54	1.8%	(4, 4)	12.573 ± 0.03	12.63	0.48%
(6, 1)	15.8 ± 0.1	15.65	0.93%	(5, 5)	16.806 ± 0.04	16.19	3.7%
(7, 2)	19.9 ± 0.1	20.11	1.1%	(6, 6)	21.278 ± 0.05	21.13	0.69%
(7, 3)	20.8 ± 0.1	21.23	2.1%	(7, 7)	25.923 ± 0.05	25.31	2.4%
(7, 4)	21.9 ± 0.1	22.42	2.4%	(8, 8)	30.876 ± 0.06	30.49	1.2%
(8, 1)	22.5 ± 0.1	22.53	0.14%	(9, 9)	35.971 ± 0.07	34.87	3.1%
(9, 1)	25.9 ± 0.1	25.97	0.27%	(10, 10)	41.302 ± 0.08	40.54	1.8%
(9, 2)	26.6 ± 0.1	26.73	0.5%	(11, 11)	46.889 ± 0.09	45	4%
(9, 3)	27.2 ± 0.1	27.55	1.3%	(12, 12)	52.624 ± 0.2	51.23	2.7%
(9, 5)	30 ± 0.1	30.77	2.6%	(13, 13)	58.545 ± 0.18	56.25	3.9%
(10, 1)	29.4 ± 0.1	29.41	0.034%	(14, 14)	64.388 ± 0.31	62.52	2.9%
(10, 2)	29.9 ± 0.1	30.05	0.52%	(15, 15)	70.927 ± 0.3	68.72	3.1%
(10, 6)	35 ± 0.1	35.93	2.7%	(1, 0)	1.5 ± 0.0	1.5	0%
(20, 1)	73.78 ± 0.01	73.83	0.061%	(2, 1)	4.281 ± 0.004	4.417	3.2%
(20, 4)	73.79 ± 0.01	74.01	0.3%	(3, 2)	7.61 ± 0.01	7.602	0.1%
(20, 10)	81.7 ± 0.1	82.57	1.1%	(4, 3)	11.362 ± 0.02	11.31	0.49%
(20, 20)	109.7 ± 0.1	113.8	3.7%	(7, 6)	24.787 ± 0.09	24.04	3%
(35, 4)	154 ± 0.1	154.1	0.078%	(11, 10)	45.474 ± 0.15	43.98	3.3%
(35, 10)	158.2 ± 0.1	158.6	0.27%	(15, 14)	69.126 ± 0.31	62.55	9.5%
(35, 20)	178.6 ± 0.1	180.4	1%				

EOS for spin polarized systems



Red line: Larkin-Ovchinnikov phase (unitary Fermi supersolid)

Black line: normal part of the energy density

Blue points: DMC calculations for normal state, Lobo et al, PRL 97, 200403 (2006)

Gray crosses: experimental EOS due to Shin, Phys. Rev. A 77, 041603(R) (2008)

$$E(n_a, n_b) = \frac{3}{5} \frac{(6\pi^2)^{2/3} \hbar^2}{2m} \left[n_a g\left(\frac{n_b}{n_a}\right) \right]^{5/3}$$

**Bulgac and Forbes,
Phys. Rev. Lett. 101, 215301 (2008)**

Formalism for Time-Dependent Phenomena

“The time-dependent density functional theory is viewed in general as a reformulation of the exact quantum mechanical time evolution of a many-body system when only one-body properties are considered.” <http://www.tddft.org>

A.K. Rajagopal and J. Callaway, Phys. Rev. B 7, 1912 (1973)

V. Peuckert, J. Phys. C 11, 4945 (1978)

E. Runge and E.K.U. Gross, Phys. Rev. Lett. 52, 997 (1984)

$$E(t) = \int d^3r \left[\varepsilon(n(\vec{r}, t), \tau(\vec{r}, t), \mathbf{v}(\vec{r}, t), \underline{\vec{j}}(\vec{r}, t)) + V_{ext}(\vec{r}, t)n(\vec{r}, t) + \dots \right]$$
$$\left\{ \begin{array}{l} i\hbar \frac{\partial u_i(\vec{r}, t)}{\partial t} = [h(\vec{r}, t) + V_{ext}(\vec{r}, t) - \mu]u_i(\vec{r}, t) + [\Delta(\vec{r}, t) + \Delta_{ext}(\vec{r}, t)]v_i(\vec{r}, t) \\ i\hbar \frac{\partial v_i(\vec{r}, t)}{\partial t} = [\Delta^*(\vec{r}, t) + \Delta_{ext}^*(\vec{r}, t)]u_i(\vec{r}, t) - [h(\vec{r}, t) + V_{ext}(\vec{r}, t) - \mu]v_i(\vec{r}, t) \end{array} \right.$$

For time-dependent phenomena one has to add currents.

Galilean invariance determines the dependence of the functional on currents.

For spin excitations one needs to introduce spin densities and currents.

TDSLDA equations in full glory

$$i\hbar \frac{\partial}{\partial t} \begin{pmatrix} \mathbf{u}_{n\uparrow}(\vec{r}, t) \\ \mathbf{u}_{n\downarrow}(\vec{r}, t) \\ \mathbf{v}_{n\uparrow}(\vec{r}, t) \\ \mathbf{v}_{n\downarrow}(\vec{r}, t) \end{pmatrix} = \begin{pmatrix} \hat{h}_{\uparrow\uparrow}(\vec{r}, t) - \mu & \hat{h}_{\uparrow\downarrow}(\vec{r}, t) & 0 & \Delta(\vec{r}, t) \\ \hat{h}_{\downarrow\uparrow}(\vec{r}, t) & \hat{h}_{\downarrow\downarrow}(\vec{r}, t) - \mu & -\Delta(\vec{r}, t) & 0 \\ 0 & -\Delta^*(\vec{r}, t) & -\hat{h}_{\uparrow\uparrow}^*(\vec{r}, t) + \mu & -\hat{h}_{\uparrow\downarrow}^*(\vec{r}, t) \\ \Delta^*(\vec{r}, t) & 0 & -\hat{h}_{\downarrow\uparrow}^*(\vec{r}, t) & -\hat{h}_{\downarrow\downarrow}^*(\vec{r}, t) + \mu \end{pmatrix} \begin{pmatrix} \mathbf{u}_{n\uparrow}(\vec{r}, t) \\ \mathbf{u}_{n\downarrow}(\vec{r}, t) \\ \mathbf{v}_{n\uparrow}(\vec{r}, t) \\ \mathbf{v}_{n\downarrow}(\vec{r}, t) \end{pmatrix}$$

Basic Numerical and Computational Details

- The system is placed on a large 3D spatial lattice, Discrete Variable Representation of wave functions (this insures both UV and IR cutoff exponential convergence)
- Derivatives are computed with FFTW/CUFFT (this insures machine accuracy) and is very fast
- Fully self-consistent treatment with fundamental symmetries respected (isospin for nuclear systems, gauge, Galilean, rotation, translation, parity)
- Adams-Bashforth-Milne 5th order predictor-corrector-modifier integrator (effectively 6th) or operator-split method, with an enhancement to ensure that time-reversal symmetry is satisfied
- No symmetry restrictions
- Number of non-linear coupled 3D+1T PDEs is of the order of the number of spatial lattice points
 - from 10,000s to a fraction of 1,000,000 determined by the dimension of the Hilbert space

$$\propto 4 \left(\frac{2p_c L}{2\pi\hbar} \right)^3 = 4N_x N_y N_z$$

- Initial state is the ground state of the SLDA (formally like HFB/BdG)
- The code was implemented on Jaguar, Titan, Franklin, Hopper, Edison, Hyak, Athena
- Initially Fortran 90, 95, 2003 ..., presently C, and obviously MPI, pthreads, etc. CUDA using GPUs
- Strong scaling down to single qpwf per MPI process; bottleneck – global reduction; advanced use of Lustre for I/O and stop/restart,

Time propagation

Equation(s) to be solved numerically: $\frac{dy(t)}{dt} = f(t)$

$y(t)$ - stands for a vector representing the values of all qpws at all points in space

Discretize time t_1, t_2, t_3, \dots

$y_n \equiv y(t_n), f_n \equiv f(t_n), \dots$

Adams-Bashforth-Milne method

(effectively 6th order, minimizes discretization and roundoff errors)

$$p_{n+1} = \frac{y_n + y_{n-1}}{2} + \frac{\Delta t}{48} (119 f_n - 99 f_{n-1} + 69 f_{n-2} - 17 f_{n-3})$$

$$m_{n+1} = p_{n+1} - \frac{161}{170} (p_n - c_n)$$

$$c_{n+1} = \frac{y_n + y_{n-1}}{2} + \frac{\Delta t}{48} (17 m_{n+1} + 55 f_n + 3 f_{n-1} + f_{n-2})$$

$$y_{n+1} = c_{n+1} + \frac{9}{170} (p_{n+1} - c_{n+1})$$

Only 2 evaluations (shown in red) of the right-hand side per step

Size of the problem (present):

- Spatial lattice size $N_x N_y N_z \approx 32^3 \dots 64^3$
- 4-component quasiparticle (complex) wave functions
- Number of quasiparticle wave functions $\approx N_x N_y N_z / 2$
- Number of bytes per time step to represent qpwfs $\approx \underline{2 \times 10^{12}}$
total memory required (wfs, TD derivatives, potentials, etc.) $\approx \underline{50 \times 10^{12}}$
- Number of time-steps $\approx O(10^6)$

This is one of the largest Direct Numerical Simulation problems ever attempted and requires capability computing

Theoretical peak on 4096 nodes on Titan (maximum number of nodes 18,688):

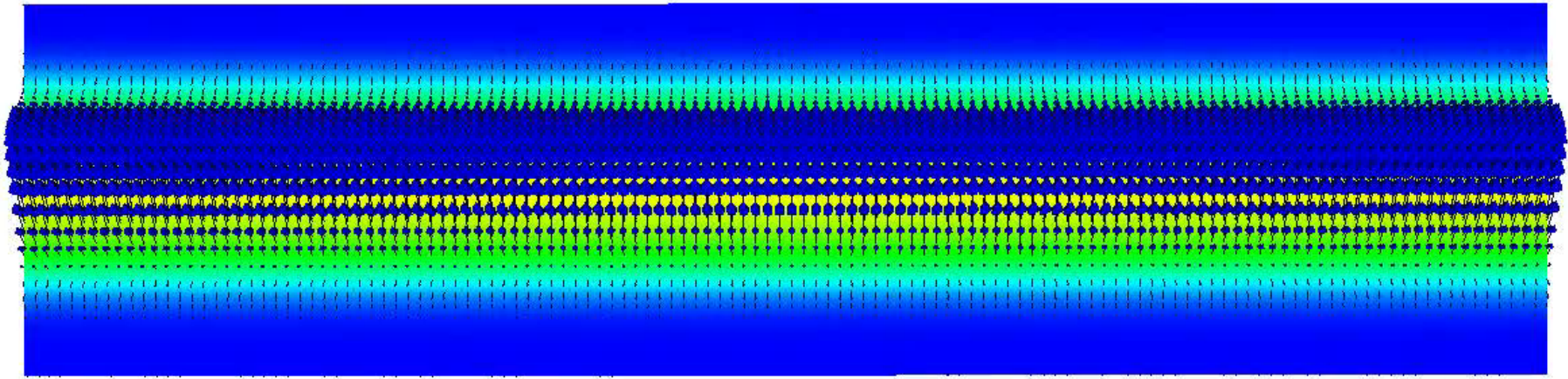
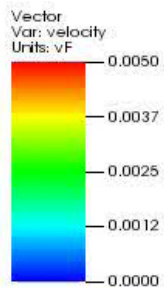
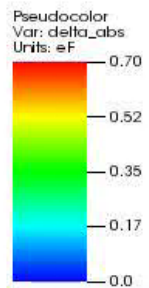
$$\underline{5.942 \text{ Petaflops}} = \underline{5.366 \text{ Petaflops (GPUs)}} + 0.576 \text{ Petaflops (CPUs)}$$

Measured speed-up GPUs (hybrid code) vs CPU (distributed memory): 16.5

261,144 nonlinear coupled 3D+1 PDEs on 64^3 spatial lattice, on 4096 nodes on Titan

Why? Hybrid MPI+CUDA. Only I/O and global reductions on CPUs. Better utilization of FP units on GPUs for CUFFT, use of batches, threads, Gemini network fast, partial reduction performed on GPUs, less data transfer between nodes

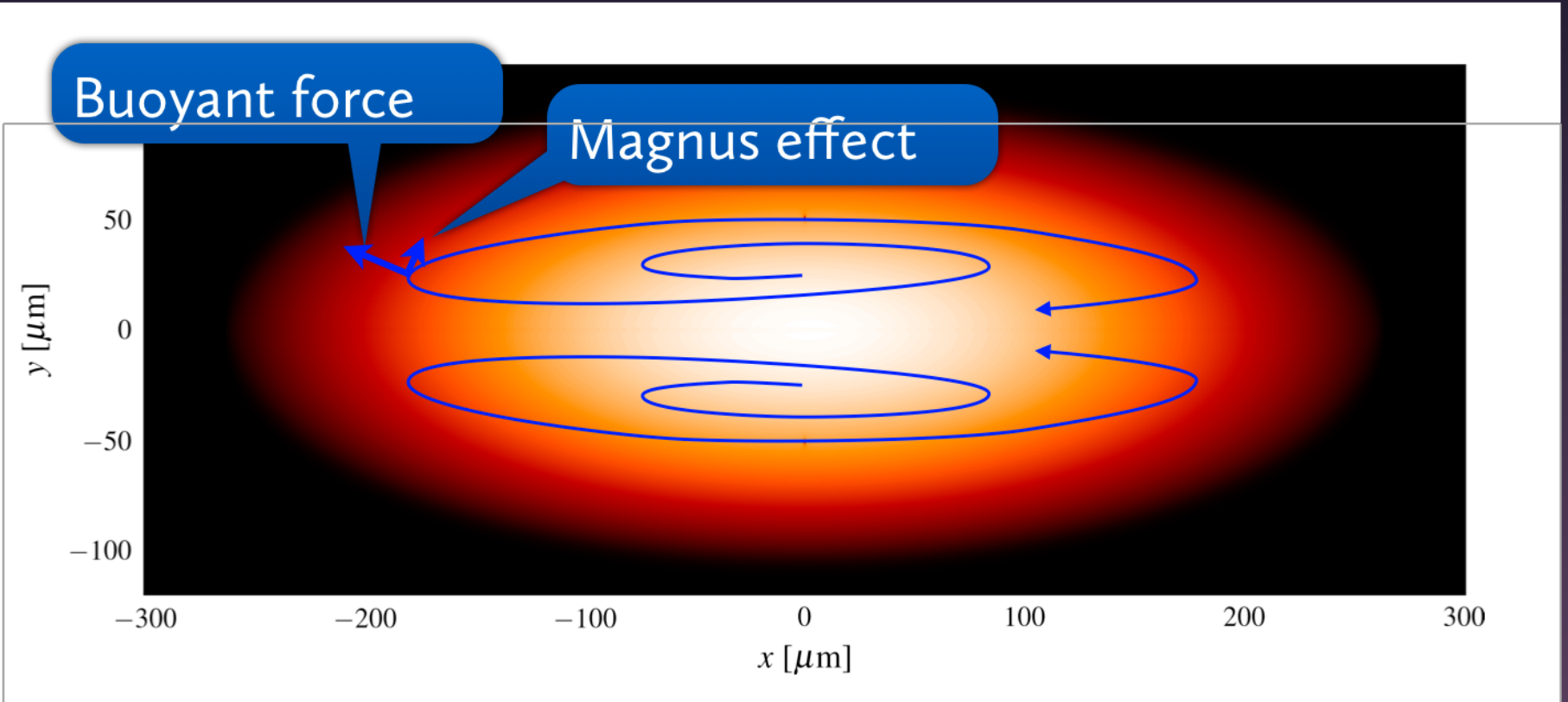
TDSLDA



Time*eF=0.0

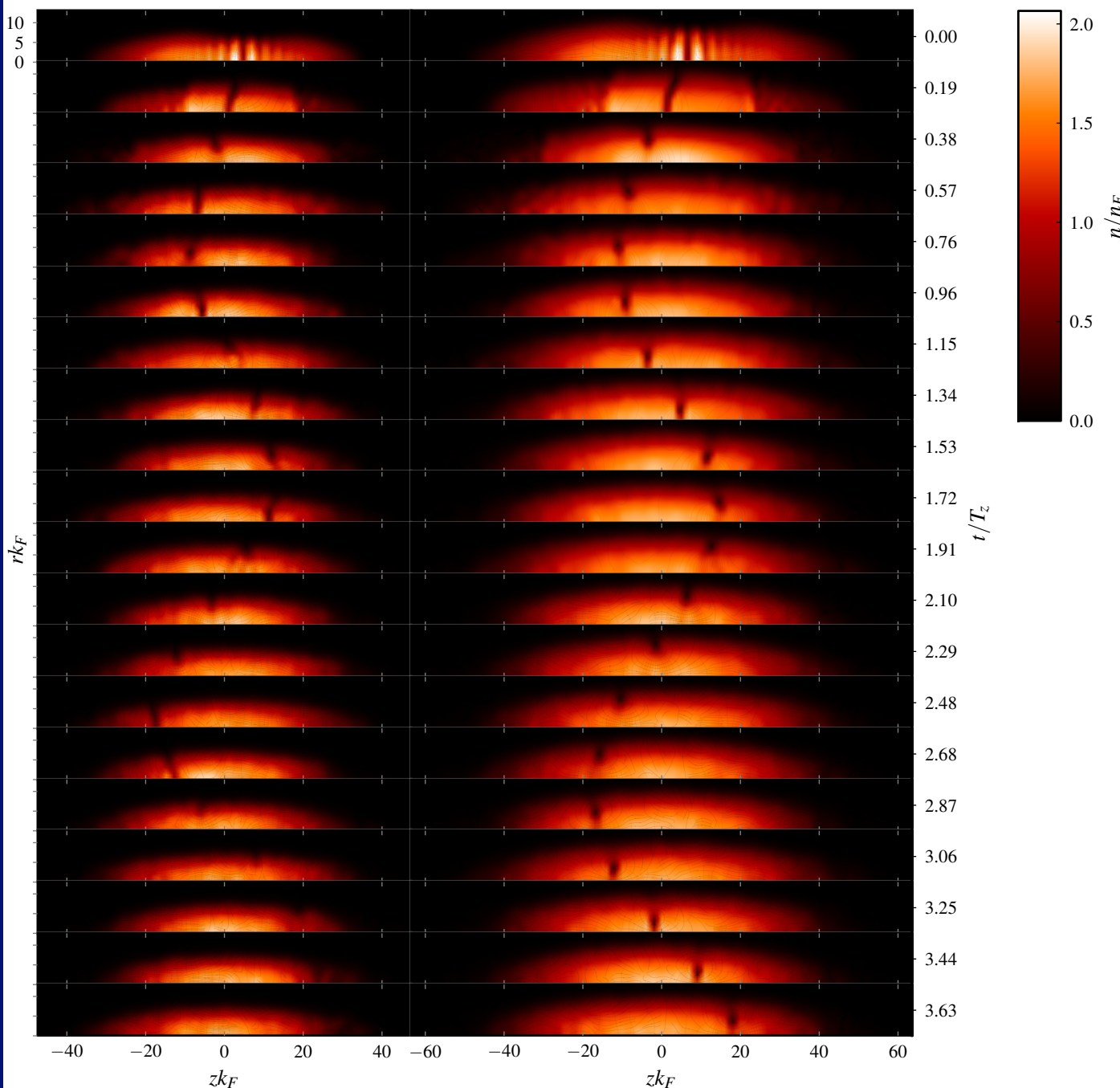
- Construction of ground state (adiabatic switching with quantum friction), generation of a domain wall using an optical knife, followed by the spontaneous formation of a vortex ring.
- Approximately 1270 fermions on a 48x48x128 spatial lattice, $\approx 260,000$ complex PDEs, $\approx 309,000$ time-steps, 2048 GPUs on Titan, 27.25 hours of wall time (initial code)

Vortex Ring Motion



Vortex ring motion (here in the presence of “thermal” noise, hence the inverse decay)

TDSLDA



Very narrow trap

Wider trap

Vortex rings

$$E \approx \frac{mn\kappa^2}{2} R \ln \frac{R}{l_{coh}}, \quad \kappa - \text{circulation}$$

$$p \approx mn\kappa\pi R^2$$

$$v = \frac{dE}{dp} \approx \frac{\kappa}{4\pi R} \ln \frac{R}{l_{coh}}$$

The bigger the vortex ring is the slower it moves

Extended Thomas-Fermi model

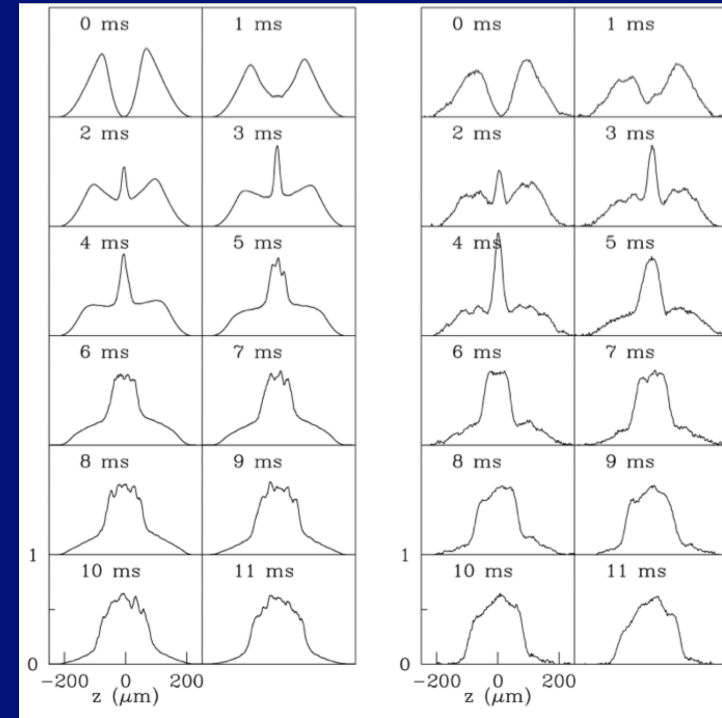
(simulate larger systems)

$$i\hbar \frac{\partial \Psi}{\partial t} = -\frac{\hbar^2}{4m} \vec{\nabla}^2 \Psi + 2 \frac{\partial E_h(n,a)}{\partial n} \Psi + 2V_{ext} \Psi$$

$$E_h(n,a) = \frac{3}{5} \varepsilon_F n \xi \frac{\xi + x}{\xi + x(1 + \zeta) + 3.0\pi\xi x^2} - \frac{\hbar^2}{2ma^2} n, \text{ accurate for } a \geq 0$$

where

$$x = \frac{1}{k_F a}, \quad n = \frac{k_F^3}{3\pi^2} = |\Psi|^2, \quad \varepsilon_F = \frac{\hbar^2 k_F^2}{2m}, \quad \zeta = 0.901 \text{ (contact)}$$



Extended TF: Anciloto, Salasnich, and Toigo, Phys. Rev. 85, 063612 (2012)

Versus

Experiment: Joseph, Thomas, Kulkarni, Abanov Phys. Rev. Lett. 106, 150401 (2011)

- Accurate Equation of State state for $a > 0$, speed of sound, phonon dispersion, static Response, respects Galilean invariance

- Ambiguous role played by the “wave function,” as it describes at the same time both the number density and the order parameter.

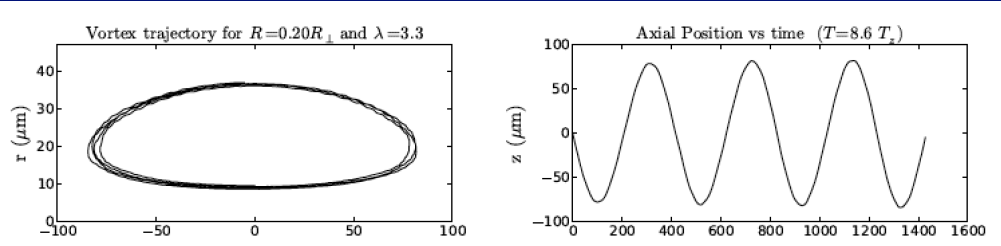
- Density depletion at vortex/soliton core exaggerated!
- Systematically underestimates time scales by a factor of close to 2

TABLE I. Dependence of the oscillation period on aspect ratio for a vortex ring imprinted with $R_0 = 0.30R_{\perp}$ at resonance. Note that the ETF consistently underestimates the period by about a factor of 0.56.

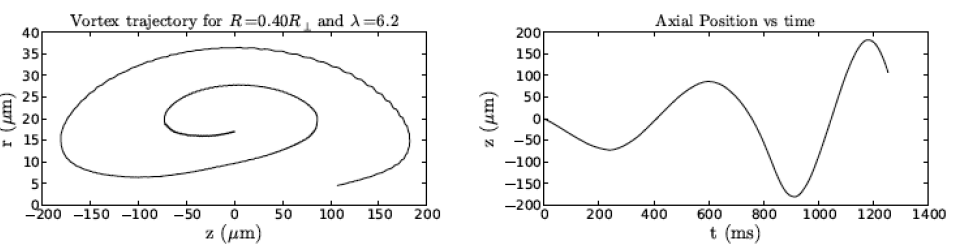
Aspect ratio	ETF period	Observed period [18]
$\lambda = 3.3$	$T = 9.9T_z$	$T = 18(2)T_z$
$\lambda = 6.2$	$T = 8.4T_z$	$T = 14(2)T_z$
$\lambda = 15$	$T = 6.7T_z$	$T = 12(2)T_z$

TABLE II. Benchmark of the ETF periods to the SLDA periods for sizes $24 \times 24 \times 96$, $32 \times 32 \times 128$, and $48 \times 48 \times 128$.

Size	T_{ETF}	T_{SLDA}	$T_{\text{SLDA}}/T_{\text{ETF}}$
$24 \times 24 \times 96$	$1.4T_z$	$1.7T_z$	1.2
$32 \times 32 \times 128$	$1.6T_z$	$1.9T_z$	1.2
$48 \times 48 \times 128$	$1.9T_z$	$2.6T_z$	1.4



Near harmonic motion close to $T=0$
(very small number of phonons)



Anti-damping of the motion in the presence
of a considerable number of phonons



TDSLDA (movie)

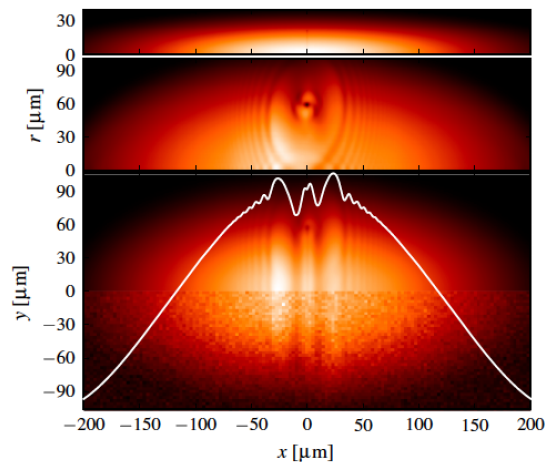
Imaging the vortex ring in experiment (movie)



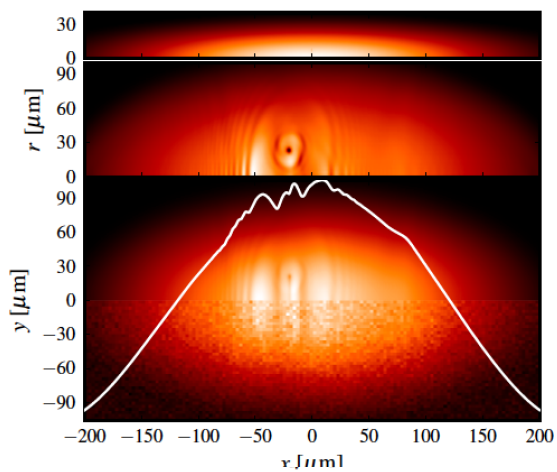
Large ring

Small ring

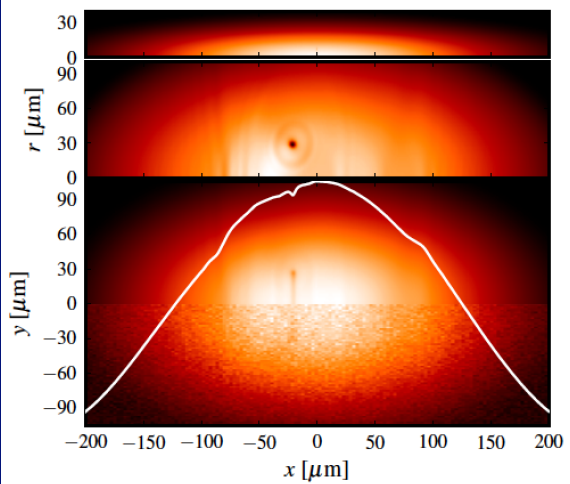
Too large B_{\min}



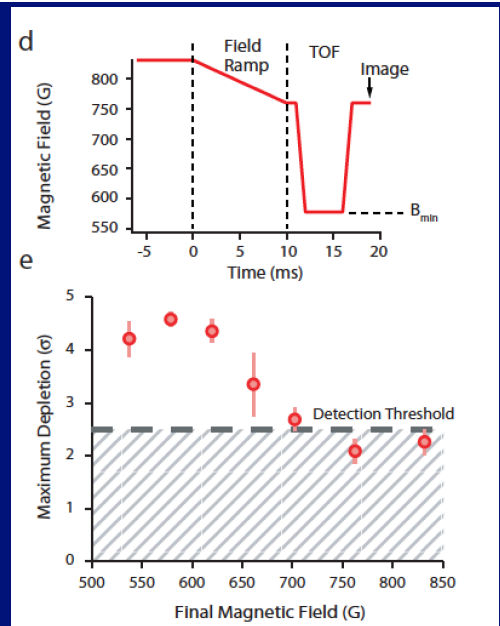
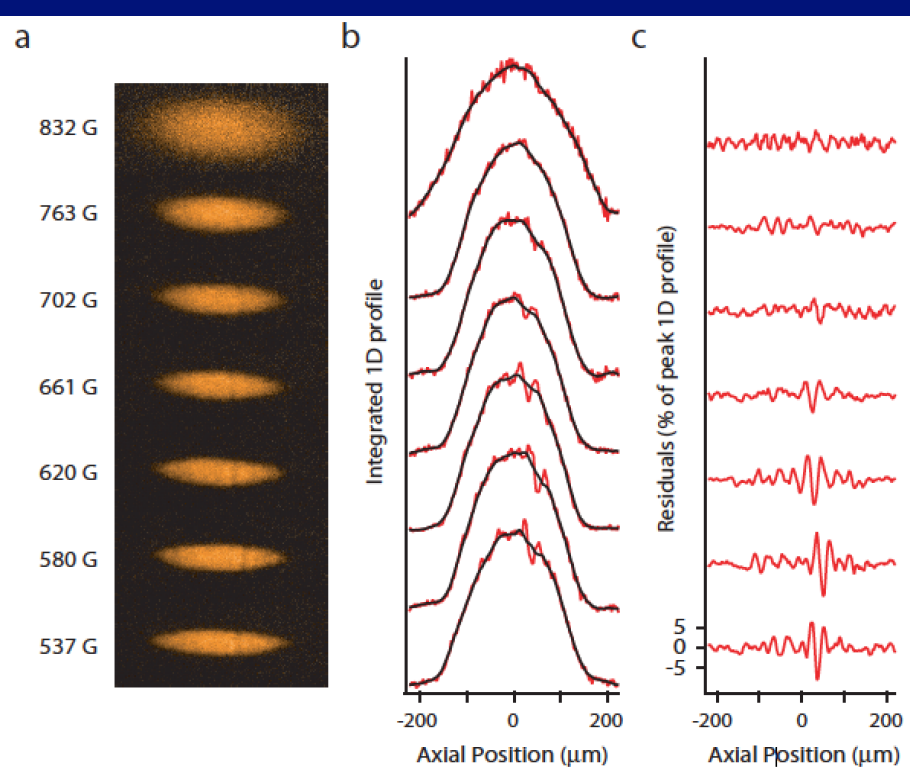
Large ring



Small ring



Insufficient ramping
of magnetic field

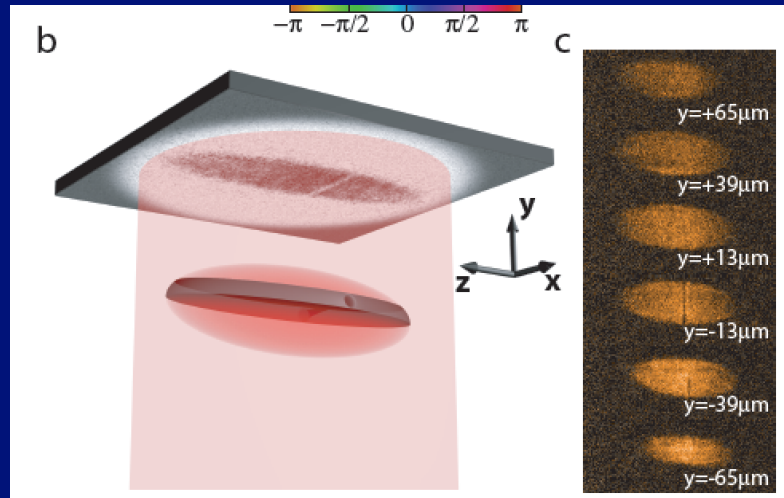


The 2014 MIT experiment:

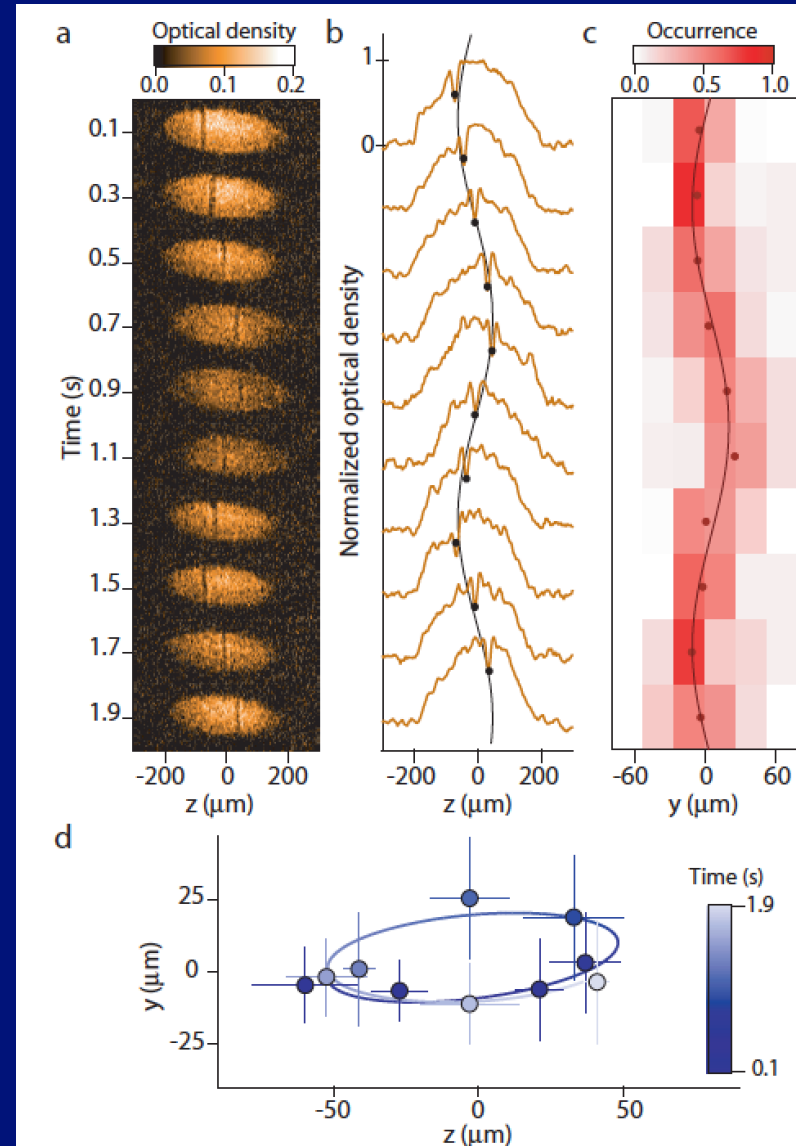
Motion of a Solitonic Vortex in the BEC-BCS Crossover

Ku, Ji, Mukherjee, Guardado-Sanchez, Cheuk, Yefsah, Zwierlein

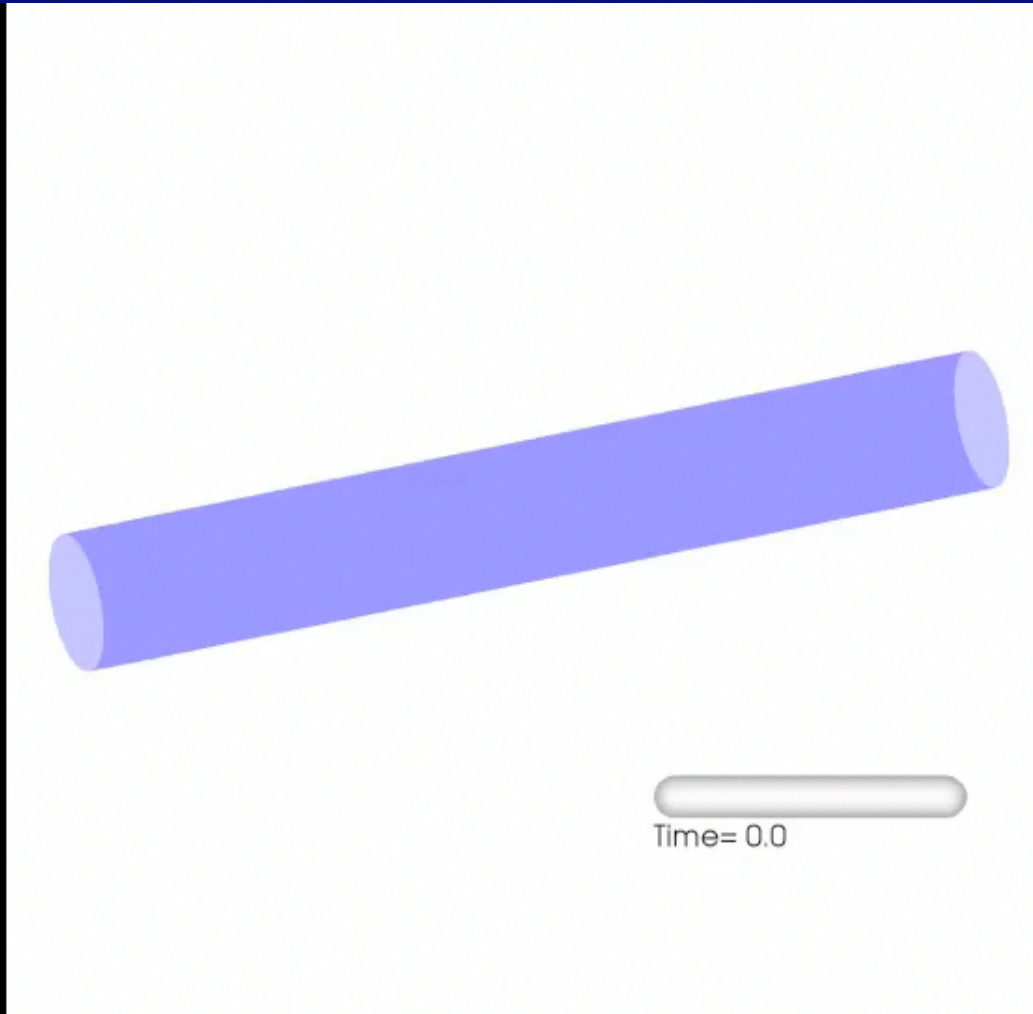
arXiv:1402.7052, 2/26/2014



- In this case the trap is triaxial, the long and medium axes horizontal
- The excitation in this case has the width of a vortex line (it is not wide as it was in the previous experiment, different imaging procedure) and it is a horizontal vortex aligned with the medium axis
- The period is again much larger than that of a domain wall
- Motion is again almost harmonic and the trajectory is very similar to that of the vortex ring



Geometry is essential! Here vortices are excited when axial symmetry is present (as in the 2013 MIT experiment)

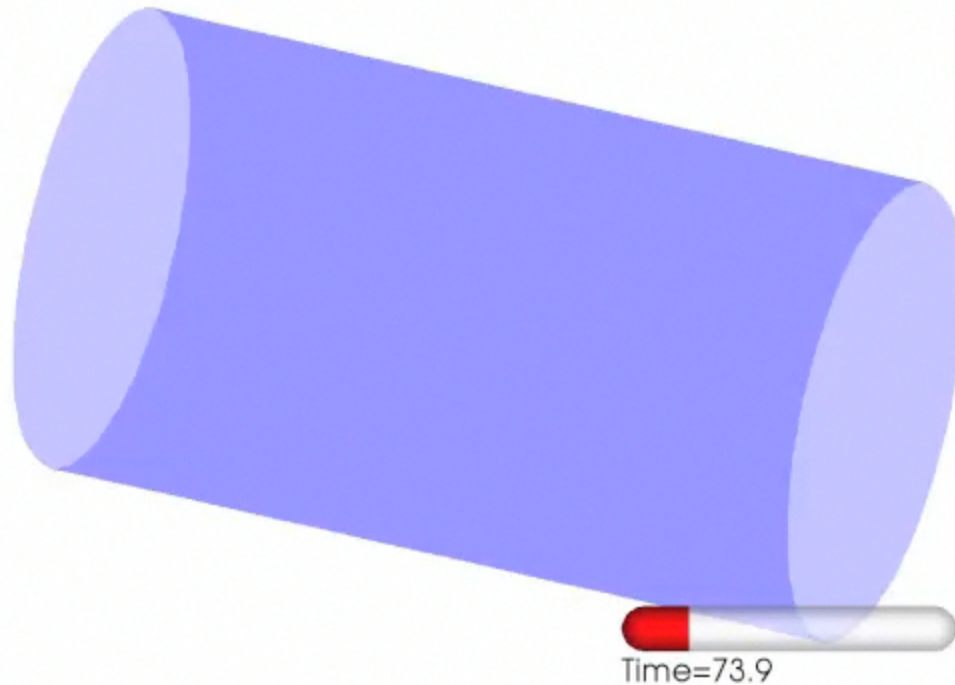


Movie

See online supplemental material to Bulgac, Luo, Magierski, Roche, and Yu, *Science*, 332, 1288 (2011)

<http://www.phys.washington.edu/groups/qmbnt/UFG/>

Here axial symmetry is slightly broken!



Movie

See online supplemental material to Bulgac, Luo, Magierski, Roche, and Yu,
Science, 332, 1288 (2011)

<http://www.phys.washington.edu/groups/qmbnt/UFG/>

What TDSLDA tells us in the case of an axially non-symmetric trap, similar to the 2014 MIT experiment? (movie)



In agreement with the new experiment, when axial symmetry is broken a domain wall, converts to a vortex ring, which shortly becomes a vortex line.



**View along the long axis
(y-axis vertical, movie)**



**In a slightly different geometry
one can put directly in evidence
in great detail the crossing and
reconnection of vortex lines, the
mechanism envisioned by Feynman
in 1955 as the route to Quantum
Turbulence (movie)**

Conclusions

Virtually all aspects of both MIT experiments (2013, 2014) are explained by vortices:

Full description of the entire experiment, starting with phase imprinting, following the dynamics of the excitations, and the imaging procedure:

- *The birth, life and death of vortices*
- *The slowness of the dynamics*
- *The dependence on the aspect ratio*
- *The role of trap geometry*
- *The anti-damping at finite temperatures*
- *The peculiarities of the imaging protocol, the role of magnetic field ramping and of the expansion*
- *The experiment provides a very strong validation of TDSLDA*
- *Demonstrated how one can now directly visualize the emergence of Quantum Turbulence envision by Feynman (1955)*

- *TDSLDA incorporates dissipation (so called one-body dissipation, equivalent to Landau Damping and Cooper pair braking)of the collective mode into non-collective ones, unlike the ETF approach*

- *Highly efficient use of GPUs on Titan to solve an extremely large system of 3D+1*